All-Atom Models for the Non-Nucleoside Binding Site of HIV-1 Reverse Transcriptase Complexed with Inhibitors: A 3D QSAR Approach†

Rick Gussio,‡ Nagarajan Pattabiraman,*,‡ Daniel W. Zaharevitz,§ Glen E. Kellogg,⊥ Igor A. Topol,‡ William G. Rice,§ Catherine A. Schaeffer,§ John W. Erickson,‡,|| and Stanley K. Burt‡,||

Frederick Biomedical Supercomputing Center, Structural Biochemistry Program, and Developmental Therapeutics Program, National Cancer Institute-FCRDC, SAIC Frederick, P.O. Box B, Frederick, Maryland 21702, and Department of Medicinal Chemistry, School of Pharmacy, Virginia Commonwealth University, Richmond, Virginia 23298

Received October 25, 1995⊗

Several molecular modeling techniques were used to generate an all-atom molecular model of a receptor binding site starting only from Ca atom coordinates. The model consists of 48 noncontiguous residues of the non-nucleoside binding site of HIV-1 reverse transcriptase and was generated using a congeneric series of nevirapine analogs as structural probes. On the basis of the receptor−ligand atom contacts, the program HINT was used to develop a 3D quantitative structure activity relationship that predicted the rank order of binding affinities for the series of inhibitors. Electronic profiles of the ligands in their docked conformations were characterized using electrostatic potential maps and frontier orbital calculations. These results led to the development of a 3D stereoelectronic pharmacophore which was used to construct 3D queries for database searches. A search of the National Cancer Institute's open database identified a lead compound that exhibited moderate antiviral activity.

Introduction

Reverse transcriptase (RT) is an important target for AIDS antiviral drug therapies. This enzyme is inhibited by nucleoside analogs which function as chain terminators of newly synthesized proviral DNA during its transcription from viral RNA. Nucleoside analogs such as AZT, ddI, and ddC have already demonstrated clinical efficacy;[1] however, their usefulness has been limited due to toxic side effects and the emergence of drug resistant HIV-1 strains.[2] Non-nucleoside RT inhibitors (NNRTIs) comprise a structurally diverse class of potent antiviral agents that usually exhibit noncompetitive inhibition and bind at a unique site on the structure of HIV-1 RT.[2] The high specificity of NNRTIs for HIV-1 RT over the cellular polymerases results in their diminished toxicity relative to nucleoside analogs.[2] Moreover, the NNRTIs can act synergistically with other classes of antiviral agents such as AZT, interferon, or CD4 immunoadhesin.[4] While NNRTIs often exhibit good antiviral efficacy in HIV-1 infected individuals, they rapidly select for mutant strains of virus.[5]

Knowledge of the detailed interactions between the NNRTIs and the non-nucleoside binding site (NNBS) should provide a structural explanation for resistance and facilitate the structure-based drug design of RT inhibitors. At the initiation of the project, only a low-resolution (2.9 Å) structure of RT complexed with nevirapine (referred to as RT-N in this paper) was published.[6] For this reason, a molecular modeling strategy[7,8] was devised to generate a reliable, all-atom molecular model of the NNBS of RT. We used the available C-α coordinates of RT−N and a panel of nevirapine analogs with known structure−activity relationships[9] as structural probes. Our method produced a reasonably accurate and complete three-dimensional atomic structure of the nevirapine binding site and was used to generate binding site models for other NNRTIs. Furthermore, our method may be useful for modeling receptor binding site structures when only limited structural data are available.

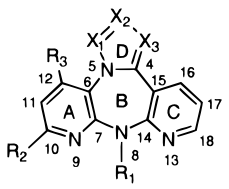

Ligand	X_1	X_2	X_3	R_1	R_2	R_3
1 (UK-129,485)	C-CH_3	C-H	N	CH_2CH_3	OCH_3	H
2	C-H	C-H	N	CH_2CH_3	OCH_3	H
3	C-CH_3	C-H	N	CH_2CH_3	H	H
4	C-H	C-H	N	CH_2CH_3	H	CH_3
5	C-H	C-H	N	C_3H_5	H	CH_3
6	C-CH_3	C-H	N	CH_2CH_3	$N(CH_3)_2$	H
7	C-CH_3	C-H	N	CH_2CH_3	NC_5H_8	H
8	C-H	C-H	N	CH_2CH_3	NC_5H_8	H
9	C-H	C-H	N	CH_2CH_3	$N(CH_3)_2$	H
10	C-CH_3	C-CH_2CH_3	N	CH_2CH_3	H	H
11 (Nevirapine)	H		O	C_3H_5	H	CH_3
12	H		O	CH_2CH_3	H	CH_3
13	C-H	C-CH_3	N	CH_2CH_3	H	H
14	C-H	C-CH_3	N	CH_2CH_3	H	H
15	C-CH_3	N	N	C_3H_5	H	H
16[a]	C-CH_3	C-H	N	CH_2CH_3	=O	CH_3
17[a]	C-CH_3	C-H	N	C_3H_5	=O	CH_3

a The nitrogen atom N9 in the A ring is protonated and bond 10 and 9 is single bonded.

Figure 1. The chemical structures of the congeneric series used in our study.

Generation of All-Atom Model for the NNBS

Initial Modeling of the NNBS. Development of an all-atom model of the RT NNBS was based on the 2.9 Å resolution crystal structure for the RT−nevirapine complex (PDB reference code is 2HVT).[6,10,11] Coordinates of this structure were available for only C-α atoms and did not include nevirapine. A model for the nevirapine structure (compound **11** in Figure 1) was built

* To whom correspondence should be addressed.
† Presented at the 208th Proceedings of the American Chemical Society.
‡ Frederick Biomedical Supercomputing Center, NCI−SAIC.
§ Developmental Therapeutics Program, NCI−SAIC.
⊥ Virginia Commonwealth University.
|| Structural Biochemistry Program, NCI−SAIC.
⊗ Abstract published in *Advance ACS Abstracts,* March 15, 1996.

0022-2623/96/1839-1645$12.00/0

using the crystal structure of nevirapine.[12] Although the nevirapine molecule is not chiral, it does possess a chirotopic N center (N11) which enables the cyclopropyl group to be either *syn* or *anti* with respect to the diazapinone ring. We reflected the *syn* conformation of the crystal structure to *anti* for the initial docking conformation. The NNBS of the RT structure was defined as consisting of 48 noncontiguous residues that surrounded the bound nevirapine molecule within a 10 Å cutoff and included the catalytic aspartyl triad (residues 110, 185, and 186). To model the complete backbone and side chain atoms for the NNBS, we searched the PDB for proteins that contained C-α coordinates of peptide fragments that were homologous in structure (within 0.2 Å rms deviation) to four consecutive C-α atoms in the NNBS of RT−N. Side chains were modeled using the frequently observed rotomers found in PDB structures. The coordinates of the resulting all-atom model were energy-minimized using the AMBER program[13] keeping the C-α atoms fixed to their crystallographic positions. The side chain atoms were manually readjusted followed by energy minimization until the resulting NNBS model was similar upon visual inspection to the published structure (Figure 1 in Smerdon *et al.*[6]). Energy minimization was performed using the DISCOVER program's cff91 force field[14] while keeping the coordinates of the C-α atoms fixed. Three bridging water molecules between nevirapine and the NNBS were added on the basis of reported data.[15] One water molecule forms hydrogen bonds with the carbonyl of Leu 234 and the carbonyl of nevirapine. The second water molecule forms hydrogen bonds with the carbonyl of Lys 101 and the nitrogen atom of the C ring of nevirapine. The third water forms hydrogen bonds with the carboxylic oxygen of Glu 138 (from the P51 subunit) and the nitrogen atom of the A ring of nevirapine. Following the procedure described above, the side chains and the backbone atoms were modeled until we reproduced the stereoview of the site as close as possible to the published structure (Figure 5 in ref 6).

Development of a 3D QSAR Model. A congeneric series of nevirapine analogs was used to further define and verify the positions and orientations of the side chains of NNBS model. Nevirapine analogs (Figure 1) were chosen as the ligands upon which to develop a 3D QSAR model for two reasons. First, the imidazo[2′,3′:6,5]dipyrido[3,2-*b*:2′,3′-*e*]-1,4-diazepines and related compounds are semirigid molecules with a limited number of conformational degrees of freedom. Secondly, the IC50 values for these compounds against HIV-RT are directly comparable since they were measured using identical assay conditions.[9] The 1-methyl,10-methoxylated analog of nevirapine (UK-129,485, compound **1** in Figure 1) is the most potent RT inhibitor of the series and was therefore used to define an initial receptor topology for the 3D QSAR model. Molecular mechanics minimizations were used to ensure reasonable geometries for the initial molecular models. The HINT[16] program was subsequently used to evaluate the resulting ligand−receptor interactions. This program quantitates individual ligand−receptor atom contacts using a hydropathic term and thereby provides a basis upon which to assess hydropathically favorable and unfavorable interactions for all ligand and receptor atom contacts. For example, our initial energy optimized model of the NNBS/UK-129,485 complex did not contain any bad nonbonded contacts. However, the results of the HINT calculations for this model showed many unfavorable interactions between hydrophobic and polar atoms. By gradually increasing the distances between the unfavorable atom pairs through the use of constrained energy minimizations, we were able to find new local minima without unfavorable hydrophobic/polar contacts. The repetition of this process over 10 simulations led to a favorable increase in the HINT total interaction constant from an initial value of 628 to a final value of 1505 without any significant change in the molecular mechanics-based energies.

The refined NNBS/UK-129,485 model served as a template for the generation of NNBS models for an additional 16 congeneric analogs (including nevirapine). For molecules other than dipyridodiazepinones, only a single bridging water molecule between the 4-imidazo nitrogen atom and the carbonyl oxygen of Leu234 was included. Docking of each of the ligands was achieved by superposition of isostructural portions of the analogs onto UK-129,485 in the NNBS pocket. The structure of each complex was then refined using the combined HINT/tethered molecular mechanics minimizations procedure in which the C-α coordinates were fixed and forces applied to the other atoms were gradually removed. The docking of all ligands was considered successful once the relative rank order of the HINT total interaction constants matched the corresponding rank order of the IC50 values for compounds in a particular subclass (see Table 1). All analogs bound in a similar fashion; in fact, the rms deviations between all compounds' atoms in the A, B, and C rings and those corresponding to the docked conformation of UK-129,-485 were less than 1 Å.

The HINT total interaction constant is the summation of hydrogen bonding, acid−acid, acid−base (AB), hydrophobic−hydrophobic (HH), base−base (BB), and hydrophobic−polar (HP) terms describing ligand−receptor atom contacts. Multiple regression methods were used to statistically model the independent contributions of each HINT term to predict IC50 values. Using an adjusted R^2 method, only four components (AB, HH, BB, and HP) of the HINT ligand−receptor total interaction constants were found to regress significantly (adjusted $R^2 = 0.85$, $F' = 20.5$, df = 4, 11, $p < 0.01$). This yielded the IC50 prediction equation:

$$\mathrm{IC50}_{\mathrm{cal}} = 15.97 + X_{\mathrm{AB}}(0.060) + X_{\mathrm{HH}}(-0.024) + X_{\mathrm{BB}}(0.083) + X_{\mathrm{HP}}(-0.024)$$

where the Xs and the $\mathrm{IC50}_{\mathrm{cal}}$ (calculated IC50) are unknown parameters. In order to test the validity of this 3D QSAR model, we calculated the IC50 value for compound **17** which was not included in the original training set. The carbonyl group of compound **17** at R2 of the A ring destroys its aromatic nature and also places a hydrophilic substituent in a hydrophobic region. The 3D QSAR model predicted an IC50 value of 20.8, which is close to the experimental IC50 value of 23.9. A complete set of atomic coordinates for our NNBS/nevirapine model (Figure 4) has been deposited with the Protein Data Bank (code is IRVO).

During the preparation of the manuscript for this paper, but after our coordinate deposition, the crystal

Table 1. HINT Calculated Total Interaction Constants and Experimental IC50 Values for HIV1-RT Activity[a]

compound	total interaction constant	IC50 (μM)
group A		
1 (UK-129,485)	1505	0.19
2	1434	0.60
group B		
3	1421	1.22
4	1404	1.62
5	1386	2.05
13	1219	11.20
group C		
6	1588	2.40
7	1449	2.70
8	1409	3.90
9	1418	3.90
group D		
10	1233	5.63
group E		
11 (nevirapine)	920	6.44
12	863	10.30
group F		
14	1127	11.20
group G		
15	1086	11.50
group H		
16	888	12.20

[a] Data taken from Terrett et al.[9] Group A: 10 methoxy-substituted imidazodipyridodiazepines. Group B: methyl-substituted imidazodipyridodiazepines. Group C: 10 amine-substituted imidazodipyridodiazepines. Group D: 1 ethyl-substituted imidazodipyridodiazepine. Group E: dipyridodiazepinones. Group F: imidazodipyridodiazepine. Group G: triazodipyridodiazepine. Group H: imidazopyridonopyridodiazepine.

coordinates of the all-atom model of the RT−N complex at 2.9 Å resolution was released (PDB code is 3HVT). Superimposition of the backbone atoms of our model on to the corresponding atoms of 3HVT yielded a rms deviation of 0.8 Å. The rms deviation between the coordinates of nevirapine in our model and in 3HVT is 0.4 Å. These deviations are well within the experimental error of independently determined protein crystal structures.[17]

Development of a Stereoelectronic Pharamacophore

We used the program DGauss[18] to perform Density Functional Theory (DFT)-based calculations of the electrostatic potentials and frontier molecular orbitals of the ligands in their docked conformations. The electrostatic potential surface for the most potent imidazodipyridodiazepine (UK-129,485) has two localized negative regions that project from hydrogen bond accepting nitrogen atoms of the C and D rings. The basicity of these two ring nitrogen atoms is reinforced by conjugation. Although we developed a 3D QSAR model with only one water molecule present for UK-129,485, the results of our quantum chemical calculations indicate that this inhibitor has the potential to accept two hydrogen bonds when bound to RT as opposed to the dipyridodiazepinones, such as nevirapine, that can form as many as three separate hydrogen bonds. DFT-based molecular orbital calculations[19] on the docked analogs illustrate that the highest occupancy molecular orbital (HOMO) for the most potent compound, UK-129,485, is well-defined and is located over the D and C rings. The lowest occupancy molecular orbital (LUMO) of UK-129,485 is located over the A ring.

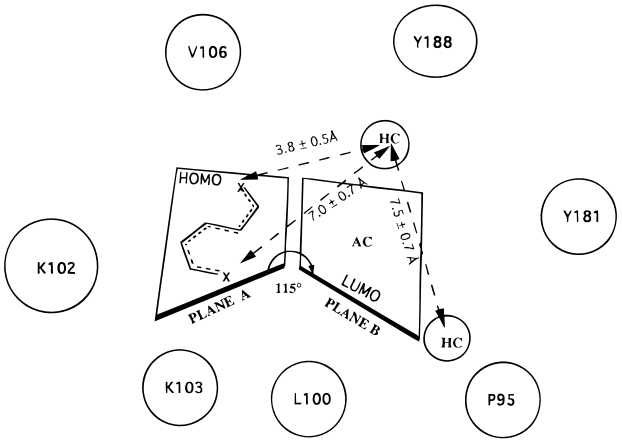

Figure 2. A 3D stereoelectronic pharmacophore developed from our docking studies. Xs denote hydrogen bond acceptor atoms HCs represent hydrocarbon centers and AC represents the aromatic center. Circles represent the exclusion spheres placed at the residues in the NNBS. The residues and their numbers are labeled inside the circles.

The refined structural and quantum mechanical descriptions of the congeneric series of NNRTIs in their NNBS-docked conformations were used to develop a 3D stereoelectronic pharamacophore (Figure 2). A major feature of this pharmacophore was the requirement of a conjugated system between two-hydrogen bonding acceptor atoms (Xs) that are all contained within plane A defined by the HOMO as described above. A second plane (referred to by B in Figure 2) formed by an aromatic center (AC), where the LUMO is located, is also essential. One of the striking features of these compounds' capacity to bind is the 115° buckle between the two planes that gives the compounds their butterfly-like shape. An additional aspect of the pharmacophore was the existence of two hydrocarbon centers (HC) at specified distances from each other and from at least one of the hydrogen-bonding heteroatoms. Schafer et al.[20] described a similar pharmacophore that was derived by comparing the structural and electronic properties with those of TIBO and nevirapine. Their pharmacophore also describes two planes, one defined with an extended π-system between two heteroatoms and the other with an aromatic center. The angle between the two planes defining the butterfly-like buckle is approximately the same in both pharmacophores. The methyl group in their pharmacophore is approximately represented by a general hydrocarbon center (HC) in ours. However, the lipophilic group that they defined above the bridge between the two planes was not included in our pharmacophore. This was due to the finding that polar groups such as a sulfone found in diaryl sulfones[21] or the amide of α-APA[22] analogs can also bind in this vicinity. Another difference between our pharmacophore and the one described by Schafer et al.[20] is that we added a second hydrocarbon center (HC) which is attached to plane B. This feature describes groups that can interact with the aliphatic portions of the residues P95 and E138 (P51 subunit). Additionally, their pharmacophore's carbonyl oxygen atom is replaced by hydrogen bond accepting heteroatoms depicted by an X in Figure 2 of our model.

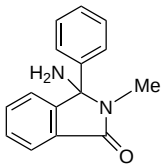

Figure 3. Chemical structure of the phenylisoindolinone (NSC119833) compound in the same orientation as the pharmacophore shown in Figure 2.

NCI Database Search

Our stereoelectronic pharmacophore was used to construct search queries for searching the National Cancer Institute's 3D open database of over 200 000 compounds.[23] The first pass identified 300 compounds that met the above search query criteria. To narrow down the number of "hits", the search queries were modified by adding exclusion spheres which correspond to steric boundaries provided by amino acid contacts of the NNBS model (Figure 2). Incorporation of the exclusion spheres proved to be a very powerful selection feature on the size and shape of the compounds and eliminated nearly 90% of the initial compounds found from the first pass. Our pharmacophore was able to include exclusion spheres because of the availability of an all-atom receptor topology which contrasts with the pharmacophore based solely on active analogs reported by Schafer et al.[20] The 33 remaining "hits" included several compounds that are known RT inhibitors, such as diaryl sulfones,[21] with 26 molecules being structurally novel and potential leads. A positive control of the search was that nevirapine was also found in the final search set.

One of the novel search hits, NSC119833 (Figure 3), a phenylisoindolinone analog, was subsequently tested against HIV-1 in CEM cells and showed moderate antiviral activity[24] with an IC50 of 10 μM. This compound was nontoxic to cells up to 800 μM and may be considered as a novel lead for RT inhibitor design. Modeling and testing of the other 25 NSC compounds are in progress. When the phenylisoindolinone motif of NSC119833 was used to search the Cambridge Crystal Database, which contains over 120 000 compounds,[27] several highly potent thiazoloisoindolinone inhibitors of RT were also found.[28]

Modeling of the NNBS for Other RT Inhibitors

On the basis of the pharmacophore described above, NNBS models were generated for three additional rigid RT inhibitors including TIBO,[29] a dihydrothiazoloisoindolinone,[30,31] and our compound, NSC119833, which was identified from NCI database searches. We developed our pharmacophore based on rigid molecules, but other more flexible inhibitors may bind to the non-nucleoside site in a modality that may not be accounted for by this pharmacophore. On the other hand, α-APA is a flexible inhibitor that can adopt the butterfly-like buckle when bound to this site. For this inhibitor, there are three rotatable bonds between two aromatic rings, but of the three, two have restricted rotations. This is due to the *o*-dichloro substitutents on one of the aromatic rings, and the possibility of an intramolecular hydrogen bond formed between the amide nitrogen of the bridge and the carbonyl oxygen atom attached to the other ring. With these conformational restrictions, we found that α-APA can adopt the butterfly-like buckle when bound to the NNBS site of RT. Our modeling results also indicate that HEPT,[32] a flexible nucleoside-like inhibitor, can bind to the NNBS by adopting the characteristic butterfly-like buckle. All-atom coordinates for these models have been deposited in the Brookhaven National Laboratory Protein Data Bank.[33] The details about the modeling of these structures will be described elsewhere.

Additional information relating to the binding modality of NNRTIs may be found in the mutations selected for by this chemically diverse group of molecules. It has been shown that the drug resistance to the NNRTIs is due to the mutations of amino acids in and around the NNBS in RT. Residues susceptible to mutation based on *in vivo* and *in vitro* investigations are A98, L100, K101, K103, V106, V108, E138, V179, Y181, Y188, and P236.[38] On examination of the contacting distances between NNRTIs and their corresponding protein residues, L100, K103, V106, Y181, Y188, W229, and L234 have direct contact with the inhibitors. It is not surprising, therefore, that two of these primary contacting residues (Y181 and L100) are the most salient mutations for NNRTIs drug resistance. Further work examining the alteration in the protein dynamics caused by these mutations needs to be carried out in order to better understand their mechanism of resistance. However, it is interesting that the mutation profiles selected

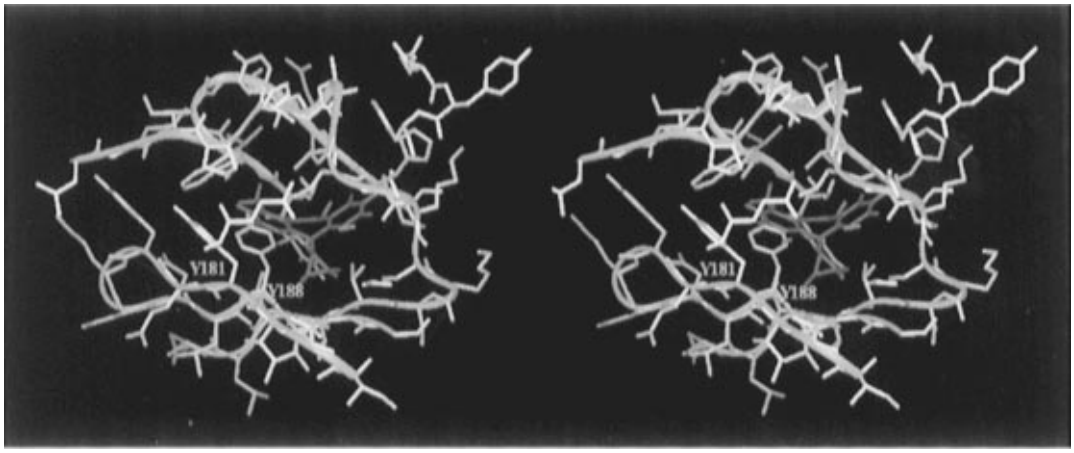

Figure 4. A stereoview of the NNBS model generated for the RT−nevirapine complex. The backbone is represented by cyan ribbons and the side chains by yellow lines. Nevirapine is represented by magenta lines. Only tyrosine residues 181 and 188 are labeled. Three water molecules are represented by green lines.

for by the various inhibitors are sometimes unique. For example, BHAP (U-90152) selects for the P236L mutation, and the pyridinone L697,593 selects for K103N with the Y181C mutation.[38] Although Y181C and L100I reduces the inhibitory activity of any of these inhibitors, their unique mutation profiles certainly support the possible existence of unique binding modalities. Future studies should examine the binding possibilities of other flexible NNRTIs such as the pyridinones[39] and the bis-heteroarylpiperazines.[40] It remains a possibility that these inhibitors may not adopt a buckled conformation upon binding and therefore would produce unique pharmacophoric information.

Conclusions

Our molecular modeling strategy successfully employed a rigid congeneric series of NNRTIs with known SAR as structural probes to develop an all-atom NNBS model. This model was generated using only the coordinates of C-α atoms from a low-resolution crystal structure. On the basis of the reliability of the resulting 3D QSAR, we deposited the coordinates of our all-atom model in the PDB prior to the release of the heavy-atom coordinates for the crystal structure of the RT−nevirapine complex.[6] On comparing our model to the crystal structure, we found that we were able to predict the correct orientation and the position of the ligand as well as that of the residues in contact with nevirapine. A stereoelectronic pharmacophore was developed using the hydropathic descriptors of the intermolecular ligand−receptor interactions and the intramolecular electronic properties calculated from their molecular orbitals. By searching the open compounds of the NCI database with queries constructed from the pharmacophore, a new lead compound possessing moderate antiviral activity was identified. On the basis of these results, we generated non-nucleoside binding site models for five additional chemically diverse NNRTIs (e.g., TIBO, HEPT). In order to evaluate the robustness of our molecular modeling strategy to do structure-based drug design/discovery, we will be applying this strategy to other potential targets.

Acknowledgment. The content of this publication does not necessarily reflect the views or policies of the Department of Health and Human Services, nor does mention of trade names, commercial products, or organization imply endorsement by the U.S. Government. We acknowledge the National Cancer Institute for allocation of computing time and staff support at the Frederick Biomedical Supercomputing Center of the Frederick Cancer Research and Development Center.

References

(1) Wilde, M. I.; Langtry, H. D. Zidovudine. An update of its pharmacodynamics and pharmacokinetic properties and therapeutic efficacy. *Drugs* **1993**, *46*, 515−578.
(2) De Clercq, E. HIV-1 specific RT inhibitors: Highly selective inhibitors of human immunodeficiency virus type 1 that are specifically targeted at the viral reverse transcriptase. *Med. Res. Rev.* **1993**, *13*, 229−258.
(3) Merluzzi, V. J.; Hargrave, K. D.; Labadia, M.; Grozinger, K.; Skoog, M.; Wu, J. C.; Shih, C.; Eckner, K.; Hattox, S.; Adams, J.; Rosehthal, A. S.; Faanes, R.; Eckner, R. J.; Koup, R. A.; Sullivan, J. L. Inhibition of HIV-1 Replication by a Nonnucleoside Reverse Transcriptase Inhibitor. *Science* **1990**, *250*, 1411−1413.
(4) Koup, R. A.; Brewster, F.; Grob, P.; Sullivan, J. L. Nevirapine synergistically inhibits HIV-1 replication in combination with zidovudine, interferon or CD4 immunoadhesin. *AIDS* **1993**, *7*, 1181−1184.
(5) Richman, D. D.; Harlir, D.; Corbeil, J.; Looney, D.; Ignacio, C.; Spector, S. A.; Sullivan, J.; Cheeseman, S.; Barringer, K.; Pauletti, D.; et al. Nevirapine resistance mutations of human immunodeficiency virus type 1 selected during therapy. *J. Virol.* **1994**, *68*, 1660−1666.
(6) Smerdon, S. J.; Jager, J.; Wang, J.; Kohlstaedt, L. A.; Chirino, A. J.; Friedman, J. M.; Rice, P. A.; Steitz, T. A. Structure of the binding site for nonnucleoside inhibitors of the reverse transcriptase of human immunodeficiency virus type 1. *Proc. Natl. Acad. Sci U.S.A.* **1994**, *91*, 3911−3915.
(7) Gussio, R.; Pattabiraman, N.; Kellogg, G. E.; Bhat, T. N.; Collins, J.; Burt, S.; Erickson, J. W. *Abstracts of Papers*, 208th National Meeting of the American Chemical Society, Washington, D.C., 1994; MEDI 34.
(8) Pattabiraman, N.; Gussio, R.; Topol, I.; Burt, S.; Erickson, J. W. *Abstracts of Papers*, 208th National Meeting of the American Chemical Society, Washington, D.C., 1994; MEDI 33.
(9) Terrett, N. K.; Bojanic, D.; Merson, J. R.; Stephenson, P. T. Imidazo[2′,3′:6,5]dipyrido[3,2-b:2′,3′-e]-1,4-diazepines: Non-nucleoside HIV-1 reverse transcriptase inhibitors with greater enzyme affinity than nevirapine. *Bioorg. Med. Chem. Lett.* **1992**, *2*, 1745−1750.
(10) Bernstein, F. C.; Koetzle, T. F.; Williams, G. J. B.; Meyer, E. F., Jr.; Brice, M. D.; Rodgers, J. R.; Kennard, O.; Shimanouchi, T.; Tasumi, M. The Protein Data Bank: A Computer-based Archival File for Macromolecular Structures. *J. Mol. Biol.* **1977**, *112*, 535−542.
(11) Abola, E. E.; Bernstein, F. C.; Bryant, S. F.; Koetzle, T. E.; Weng, J. Protein Data Bank. In *Crystallographic Databases - Information Content, Software Systems, Scientific Applications*; Allen, F. H., Bergerhoff, G., Sievers, R., Eds.; Data Commission of the International Union of Crystallography: Bonn, 1987; pp 107−132.
(12) Mui, P. W.; Jacobsen, S. P.; Hargrove, K. D.; Adam, J. Crystal structure of nevirapine, a non-nucleoside inhibitor of HIV-1 reverse transcriptase and computational alignment with a structural diverse inhibitor. *J. Med. Chem.* **1992**, *35*, 201−202.
(13) Pearlman, D. A.; Case, D. A.; Caldwell, J. C.; Seibel, G. L.; Singh, U. C.; Weiner, P. W.; Kollman, P. A. AMBER 4.0 (UCSF) Manual, 1991.
(14) Maple, J. R.; Thacher, T. S.; Dinur, U.; Hagler, A. T. Biosym force field research results in new technique for the extraction of inter- and intramolecular forces. *Chem. Design Automat. News* **1990**, *5*, 5−10.
(15) Stuart, D. I.; Ren, J. S.; Esnouf, R.; Jones, E. Y.; Ross, C.; Somers, D.; Stammers, D. K. High resolution refined structure of HIV-1 reverse transcriptase-inhibitor complexes: Implications for drug resistance. Presented in the Third International Workshop on HIV drug resistance held in Kauai, Hawaii, August 1994, p 29.
(16) Meng, E. C.; Kuntz, I. D.; Abraham, D. J.; Kellogg, G. E. Evaluating Docked complexes with the HINT exponential function and empirical atomic hydrophobicities. *J. Comput.-Aided Mol. Des.* **1994**, *8*, 299−306.
(17) Wlodawar, A.; Nachnaan, J.; Gilliland, G. L.; Gallagha, W.; Woodward, C. Structure of form III crystals of bovine pancreatic trypsin inhibitors. *J. Mol. Biol.* **1989**, *198*, 469−480.
(18) Andzelm, J. W.; Wimmer, E. J. Density functional gaussian-type-orbital approach to molecular geometries, vibrations and rotation energies. *J. Chem. Phys.* **1992**, *96*, 1280−1303.
(19) In DFT calculations, for small orbital relaxation upon ionization or electron attachment, the orbitals associated with the lowest ionization potential and highest electron affinity correspond to the HOMO and LUMO in the traditional MO theory. In this paper, we refer to these orbitals generated by DFT as HOMOs and LUMOs.
(20) Schafer, W.; Friebe, W.-G.; Leinert, H.; Mertens, A.; Poll, T.; von der Saal, W.; Zilch, H.; Nuber, B.; Ziegler, M. L. Non-nucleoside inhibitors of HIV-1 reverse transcriptase: Molecular modeling and X-ray structure investigations. *J. Med. Chem.* **1993**, *36*, 726−733.
(21) McMohan, J. B.; Gulakowski, R. J.; Weislow, O. S.; Schultz, R. J.; Narayanan, V. L.; Clanton, D. J.; Pedemonte, R.; Wassmundt, F. W.; Buckheit, R. W., Jr.; Decker, W. D.; White, E. L.; Bader, J. P.; Boyd, M. R. Diarylsulfones, a new chemical class of nonnucleoside antiviral inhibitors of human immunodeficiency virus type I reverse transcriptase. *Antimicrob. Agents Chemother.* **1993**, *37*, 754−760.
(22) Pauwels, R.; Andries, K.; Debyser, Z.; Daele, P. V.; Schols, D.; Stoffels, P.; Vreese, K. D.; Woesternborghs, R.; Vandamme, A.-M.; Janssen, C. G. M.; Anne, J.; Cauwenbergh, G.; Desmyter, J.; Heykants, J.; Janssen, M. A. C.; Clercq, E. D.; Janssen, P. A. J. Potent and hightly selective human immunodeficiency virus type 1 (HIV-1) inhibition by a series of alpha-anilinophenylacetamide derivatives targeted at HIV-1 reverse transcriptase. *Proc. Natl. Acad. Sci. U.S.A.* **1993**, *90*, 1711−1715.
(23) Milne, G. W. A.; Nicklaus, M. C.; Driscoll, J. S.; Wang, S.; Zaharevitz, D. National Cancer Institute Drug Information System 3D Database. *J. Chem. Inf. Comput. Sci.* **1994**, *34*, 1219−1224.

(24) The anti-HIV assay was performed as previously described[25,26] using the XT7 microliter assay that quantitates drug-induced protection from the killing of CEM-SS cells by HIV-1_{RF}.
(25) Weislow, O. S.; Kiser, R.; Fine, D. L.; Bader, J.; Shoemaker, R. H.; Boyd, M. R. New soluble-formazan assay for HIV-1 cytopathic effects: Application to high-flux screening of synthetic and natural products for AIDS-antiviral activity. *J. Natl. Cancer Inst.* **1989**, *81*, 577−586.
(26) Cushman, M.; Golebiewski, W. M.; McMohan, J. B.; Buckheit, B. W., Jr.; Clanton, D. J.; Weislow, O.; Haugwitz, R. D.; Bader, J.; Graham, L.; Rice, W. G. Design, synthesis, and biological evaluation of cosalane, a novel anti-HIV agent which inhibits multiple features of virus reproduction. *J. Med. Chem.* **1994**, *37*, 3040−3050.
(27) Allen, F. H.; Davies, J. E.; Galloy, J. J.; Johnson, O.; Macrae, C. F.; Mitchell, E. M.; Mitchell, G. F.; Smith, J. M.; Watson, D. G. The development of version 3 and 4 of the cambridge database system. *J. Chem. Inf. Comput. Sci.* **1991**, *31*, 187−204.
(28) Chimirri, A.; Grasso, S.; Monforte, A. M.; Monforte, P.; Zappala, M. Anti-HIV agents I. Synthesis and in vitro anti-HIV evaluation of novel 1H,3H-thiazolo[3,4-a]benzimidazoles. *Il Farmaco* **1991**, *46*, 817−823.
(29) Pauwels, R.; Andries, K.; Desmyter, J.; Schols, D.; Kukla, M. J.; Breslin, H. J.; Raeymaecjers, A.; Gelder, J. V.; Woesternborghs, R.; Heykants, J.; Schellekens, K.; Janssen, M. A. C.; Clercq, E. D.; Janssen, P. A. J. Potent and selective inhibiton of HIV-1 replication in vitro by a novel series of TIBO derivatives. *Nature* **1990**, *343*, 470−474.
(30) Maass, G.; Immendoerfer, U.; Koenig, B.; Leser, U.; Mueller, B.; Goody, R.; Pfaff, E. Viral resistance to the thiazolo-iso-indolinones, a new class of nonnucleoside inhibitors of human immunodeficiency virus type 1 reverse transcriptase. *Antimicrob. Agents Chemother.* **1993**, *37*, 2612−2617.
(31) Mertens, A.; Zilch, H.; Konig, B.; Schafer, W.; Poll, T.; Kampe, W.; Seidel, H.; Leser, U.; Leinert, H. Selective non-nucleoside HIV-1 reverse transcriptase inhibitors. New 2,3-dihydrothiazolo-[2,3-a]isoindol-5 (9bH)-ones and related compounds with anti-HIV-1 activity. *J. Med. Chem.* **1993**, *36*, 2526−2535.
(32) Baba, M.; Tanaka, H.; De Clercq, E.; Pauwels, R.; Balzarini, J.; Schols, D.; Nakashima, H.; Perno, C.-F.; Walker, R. T.; Miyasaka, T. Highly specific inhibition of human immunodeficiency virus type 1 by a novel 6-substituted acyclouridine derivative. *Biochem. Biophys. Res. Commun.* **1989**, *165*, 1375−1381.
(33) PDB codes for the NNBS models of the RT complexes: IRVL for α-APA; IRVM for HEPT; IRVN for phenylisoindolinone (NSC-119,833); IRVP for thiazoloisoindolinone; IRVQ for TIBO; and IRVR for imidazodipyridodiazepine (UK-129,485). Our docking models for nevirapine, α-APA, TIBO, and HEPT (PDB codes 1RVO, 1RVL, 1RVQ, and 1RVM, respectively) appear to be in complete agreement with the position and orientations of the reported crystal structures.[34−36] However, orientation of HEPT in our model appears to place the thymine base 180° opposite to the orientation reported.[36] In our NNBS model for TIBO, the phenyl and imidizolone rings are rotated by 160° from the observed crystal structure of the complex.[37]
(34) Ren, J.; Esnouf, R.; Garman, E.; Somers, D.; Ross, C.; Kirby, C.; Keeling, J.; Darby, G.; Jones, Y.; Stuart, D.; Stammers, D. High resolution structures of HIV-1 RT from four RT-inhibitor complexes. *Nature Struct. Biol.* **1995**, *2*, 293−302.
(35) Ding, J.; Das, K.; Moereels, H.; Koymans, L.; Andries, K.; Janssen, P. A. J.; Hughes, S. H.; Arnold, E. Structure of HIV-1 RT/TIBO R86183 complex reveals similarity in the binding of diverse nonucleoside inhibitors. *Nature Struct. Biol.* 1995, *2*, 407−415.
(36) Ding, J.; Das, K.; Tantillo, C.; Zhang, W.; Clark, A. D., Jr.; Jessen, S.; Lu, X.; Hsiou, Y.; Jacob-Molina, A.; Andries, K.; Pauwels, R.; Moereels, H.; Koymans, L.; Janssen, P. A. J.; Smith, R. H., Jr.; Koepke, M. K.; Michejda, C. J.; Hughes, S. H.; Arnold, E. Structure of HIV-1 reverse transcriptase in a complex with the non-nucleoside inhibitor α-APA R95845 at 2.8 Å resolution. *Structure* **1995**, *3*, 365−379.
(37) Ren, J.; Esnouf, E.; Hopkins, A.; Ross, C.; Jones, Y.; Stammers, D.; Stuart, D. The structure of HIV-1 reverse transcriptase complexed with 9-chloro-TIBO: lessons for inhibitor design. *Structure* **1995**, *3*, 915−926.
(38) Mellors, J. W.; Larder, B. A.; Schinazi, R. F. Mutations in HIV-1 reverse transcriptase and protease associated with drug resistance. *Int. Antiviral News* **1995**, *3*, 8−13.
(39) Goldman, M. E.; Nunberg, J. H.; O'Brien, J. A.; Quintero, J. C.; Schleif, W. A.; Fruend, K. F.; Gaul, S. L.; Saari, W. S.; Wai, J. S.; Hoffman, J. M.; Anderson, P. S.; Hupe, D. J.; Emini, E. A.; Stern, A. M. Pyridinone derivatives: Specific human immunodeficiency virus type 1 reverse tranascriptase inhibitors with antiviral activity. *Proc. Natl. Acad. Sci. U.S.A.* **1991**, *88*, 6863−6867.
(40) Romero, D. L.; Busso, M.; Tan, C.-K.; Reusser, F.; Palmer, J. R.; Poppe, S. M.; Aristoff, P. A.; Downey, K. M.; So, A. G.; Renick, L.; Tarpley, W. G. Nonnucleoside reverse transcriptase inhibitors that potently and specifically block human immunodeficiency virus type 1 replication. *Proc. Natl. Acad. Sci. U.S.A.* **1991**, *88*, 8806−8810.

JM9508088